Conjunction of thermal lens spectrometry and high-performance liquid chromatography
Approach to data treatment

Aleksandr A. Dzyabchenko, Mikhail A. Proskurnin*, Andrei G. Abroskin,
Denis V. Chashchikhin

*Analytical Chemistry Division, Chemistry Department, M.V. Lomonosov Moscow State University, Vorob'evy Gory, Moscow 119899,
GSP-3 V-234, Russia*

Abstract

Dual-beam thermal lens spectrometry (TLS) is used as a detection system in HPLC. An algorithm for chromatogram handling, which is based on fast Fourier transform, is developed. The algorithm allows a considerable increase (1.5 to 2 orders) in the sensitivity of HPLC–TLS determinations compared with HPLC with conventional spectrophotometric detection. A comparison of the methods for calculating the performance characteristics from peak heights (conventional approach) and peak areas showed that the latter gives more reliable results. The experimental set-up and developed methods were used for determination of Co and Ni in the form of their pre-synthesised chelates with 4-(2-pyridylazo)resorcinol; the limits of detection are $3 \cdot 10^{-8}$ and $1 \cdot 10^{-7}$ M, respectively.   © 1998 Published by Elsevier Science B.V. All rights reserved.

Keywords: Thermal lens spectrometry; Detection, LC; Metal chelates

1. Introduction

Conjunction of HPLC and thermal lens spectrometry (TLS) seems very promising for widening the possibilities of both methods and has already gained acceptance in analytical practice [1,2]. Application of such a high-sensitive detection method as TLS in HPLC allows a drastic increase in the limits of detection compared to conventional spectrophotometric detection [1,3].

However, one of the main disadvantages of this approach is the high sensitivity of a thermal-lens detector to fluctuations in the flow-rate of the mobile phase. Thus, this paper is devoted to studying this problem with model systems and to the methods of data treatment for compensating for the noise of the analytical signal caused by the fluctuations in the flow system.

2. Experimental

2.1. Apparatus

2.1.1. Chromatographic system

The chromatographic system included an M6000A HPLC pump (Waters, Milford, MA, USA), a stainless-steel damper of flow-rate fluctuations made in

*Corresponding author.

the laboratory, an i1001 injector for liquid chromatography (Inkrom Technoteenindus, Tallinn, Estonia) with the loop volume of 50 μl, a stainless steel column 50×4.6 mm packed with Nucleosil 10 SB (Macherey-Nagel, Duren, Germany), and a flow cell with optical pathlength of 10 mm, quartz windows, and volume of 20 μl.

The pump has two plungers working in opposite phases and an internal damper of mobile phase fluctuations. The pump provides the pressure up to 400 atm (1 atm$=101$ 325 Pa) and allows variation of the flow-rate from 0.1 to 5.0 ml min^{-1} with a step of 0.1 ml min^{-1}.

2.1.2. Thermal-lens spectrometer

The installation of a dual-beam thermal-lens spectrometer was described in detail in a previous paper [4]. It was set up with parallel dual-beam optical configuration: A pump Ar$^+$ laser (Innova 90-6, Coherent, Palo Alto, CA, USA) was operated at 488.0 and 514.5 nm, power in the cell was 40 mW. A He–Ne laser (SP 106-1, Spectra-Physics, Eugene, OR, USA; 10 mW, 632.8 nm) was exploited as a probe. The focal lengths of lenses were $f=300$ mm (the pump) and $f'=185$ mm (the probe). A change in intensity in the centre of the probe beam was measured by a photodiode detector. The voltage from the signal photodiode (proportional to the power of light) was translated to an IBM PC/AT computer with a DT-2801A ADC-DAC board (Data Translation, Marlboro, MA, USA). A change in intensity in the centre of the probe beam was measured by a photodiode detector. It was monitored by a synchronisation block connected to a synchronisation photodiode.

2.1.3. Auxiliary measurements

Spectrophotometric measurements were made using an SF-46 spectrophotometer (LOMO, St. Petersburg, Russia) with fused-quartz cells with optical pathlength of 1 cm. Measurement of pH was made by an EV-74 potentiometer (Gomel, Belarus) with a glass ion-selective electrode (precision ±5%) and a silver-chloride reference electrode. The instrument was adjusted at 25°C using standard buffer solutions of pH 2.50 and 9.18.

2.2. Reagents and procedures

2.2.1. Chemicals

The following solvents were used throughout: doubly distilled water (filtered through a 0.45-μm filter and degassed; resulting pH 5.8) and pure-grade acetonitrile (distilled using a 35-cm dephlegmator under atmospheric pressure; boiling temperature 83.0–83.5°C). Stock solutions of metals (0.01 M) were prepared using pure cobalt(II) sulfate hydrate, analytical-grade lead(II) acetate trihydrate, pure nickel(II) nitrate hexahydrate, analytical-grade ammonium iron(II) sulfate hexahydrate, analytical-grade copper(II) sulfate pentahydrate, and pure zinc(II) chloride. The stock solutions of the reagents were prepared by dissolving analytical-grade disodium salt of EDTA (0.01 M), analytical-grade sodium perchlorate (0.05 M), analytical-grade potassium hydroxide (20%), and analytical-grade sodium salt of 4-(2-pyridylazo)resorcinol (PAR, 0.002 M). All the reagents were from Reakhim (Moscow, Russia).

Stock solutions of pre-synthesised chelates were prepared by adding aqueous PAR solutions (two-fold excess amounts of the reagent) to test metal solutions ($n \cdot 10^{-5}$ M). Working solutions were prepared by diluting the stock solutions with water.

2.2.2. Procedures

Determination of the metals was made using an eluent containing 50 mM of NaClO$_4$, 1 mM of EDTA, and 40% (v/v) of acetonitrile. The eluent was prepared by mixing 80 ml of rectified acetonitrile with 20 ml of the stock solution of sodium perchlorate and 4 ml of the stock solution of EDTA followed by diluting the mixture to 200 ml and adjusting pH to 7 by two or three drops of a 20% solution of potassium hydroxide. Then, the eluent was filtered through a 0.45-μm filter and degassed.

2.3. Data handling

2.3.1. Primary software

Data calculation and preliminary manipulation was made by a laboratory-written program [4,5]. It served to detect and to handle the steady-state values of thermal lens signal; its algorithm was described in detail in [4]. This software records a chromatogram (thermal lens signal against time), checks it for

spurious points, and stores data in a file (with the parameters of detection). The software allows the operator to adjust the response time of the thermal lens spectrometer by changing the parameters of measurement (the number of points in each period of steady state of the lens, the frequency of sampling, etc.)

2.3.2. Metrological calculations

Thermal lens signal S was calculated from the equation

$$S \equiv 2.303EA = \sqrt{\frac{2(I_0 - I_\infty)}{I_\infty} + 1} - 1 \tag{1}$$

Here, I_0 and I_∞ are intensities in the probe-beam centre on a photodiode in the case of closed modulator (no thermal lens) and in the case of a stationary thermal lens, respectively; A is absorbance; and

$$E = -0.524 \cdot \frac{\mathrm{d}n/\mathrm{d}T P}{k\lambda} \tag{2}$$

is the enhancement factor. In the latter formula, $\mathrm{d}n/\mathrm{d}T$ is the temperature gradient of refractive index of the medium, P is the power of the pump laser radiation with wavelength λ, and k is thermal conductivity of the medium.

Corrected retention times were calculated as differences between the maxima of peaks of test compounds and the maximum of the injection peak.

Heights of chromatographic peaks (calculated relative to the average signal of the baseline) and their areas (calculated by numerical integration relative to the baseline) were used as analytical signals. In both cases, the chromatograms were pre-treated with the developed software (see below).

Determination of metals was made from series of solutions of pre-synthesised PAR chelates by building peak height vs. concentration or peak area vs. concentration calibration curves using samples of a single metal. The concentration ranges and the number of replicate measurements are shown in Table 1. All the calibration curves (both for heights and areas) were built by linear regression using linear square fits. The limits of detection were calculated by the 3σ-criterion.

3. Results and discussion

3.1. Flow-rate selection

A significant dependence of thermal lens signal on mobile-phase flow-rate is one of the largest problems of conjunction of optothermal detection techniques and flow analysis [6–8]. Thus, prior to gathering any analytical data, one should find the optimum conditions for thermal-lens measurements in the flow. The most important, and opposite, factors are a decrease in the sensitivity of thermal lens measurements with an increase in the flow-rate [9] and a considerable washout of the peaks at low flow-rates. Moreover, the dependence of flow-rate fluctuations on the flow-rate is individual for a certain design and components of the flow system.

We measured thermal lens signal (Fig. 1) and signal-to-noise (S/N) ratio (Fig. 2) in the range of flow-rates of 0.1–2.0 ml min^{-1} using distilled water as a mobile phase. While the dependence of the signal shows a nearly quadratic decrease with the flow-rate, the S/N dependence proved to be a sine wave with an increasing amplitude and a constant period. In our opinion, this behaviour should be

Table 1
Characteristics of chromatographic determination of cobalt and nickel as their PAR chelates using a thermal lens detector ($P = 0.95$)

Metal (replicate measurements)	Linear calibration range (M)	Peak heights			Peak areas		
		Repeatability, R.S.D. (%)	Reproducibility, R.S.D. (%)	$c_{\min \, (h)}$ (M)	Repeatability, R.S.D. (%)	Reproducibility, R.S.D. (%)	$c_{\min \, (S)}$ (M)
Co ($n=5$)	$1\cdot10^{-7}$–$5\cdot10^{-6}$	5	6	$5\cdot10^{-8}$	4	7	$3\cdot10^{-8}$
Ni ($n=3$)	$1\cdot10^{-6}$–$2\cdot10^{-5}$	6	7	$5\cdot10^{-7}$	5	7	$1\cdot10^{-7}$

Pump laser wavelength 514.5 nm; pump power in the cell 40 mW; Nucleosil 10 SB 50×4.6 mm column; flow-rate 1.2 ml min^{-1}; eluent: 50 mM NaClO$_4$, 1 mM EDTA, 40% (v/v) acetonitrile.
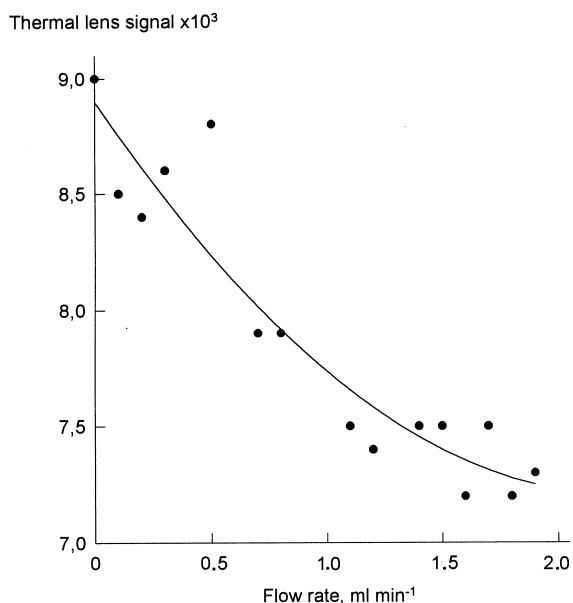
Fig. 1. Dependence of thermal-lens signal on flow-rate. Working wavelength 514.5 nm. Pump power in the cell is 40 mW. A Nucleosil 10 SB 50×4.6 mm column; eluent: mobile phase is distilled water.
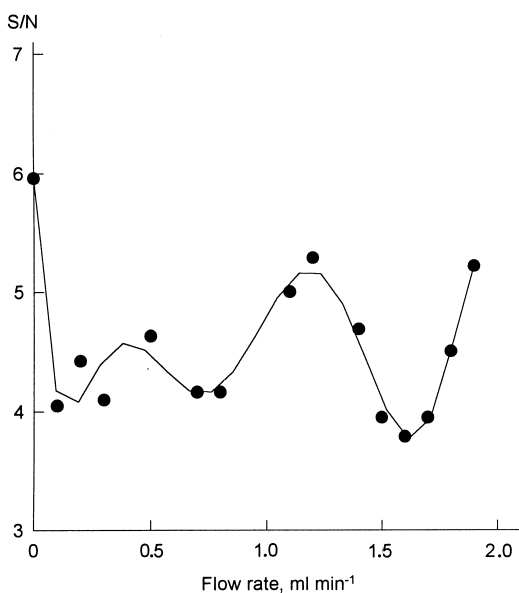

Fig. 2. Dependence of signal-to-noise ratio (S/N) on flow-rate. Working wavelength 514.5 nm. Pump power in the cell is 40 mW. A Nucleosil 10 SB 50×4.6 mm column; mobile phase is distilled water.

accounted for a minor misbalance in the work of the pump heads. The minimum misbalance corresponds to flow-rates of 0.5 and 1.2 ml min^{-1}. In the case of flow-rates over 2.0 ml min^{-1}, the S/N becomes irreproducible (this is not shown in Fig. 2). These rates were not considered due to low sensitivity of thermal-lens measurements. However, in our further experiments only the flow-rate of 1.2 ml min^{-1} was used as a working flow-rate, because the flow-rate of 0.5 ml min^{-1} did not provide satisfactory rapidity of determination of metals with PAR.

3.2. Model system selection

Selection of the model system was made for the following reasons. The substances should be well-studied by chromatography and provide sensitive detection by thermal lens spectrometry, should not require sophisticated sampling procedures and allow easy variation of experimental conditions. Thus, we selected chelates of transition metals with PAR because they meet all the above criteria [10]. The analysis of absorption spectra of PAR chelates of Co, Ni, Fe, Pb and Cu allowed us to choose the wavelength of 514.5 nm for thermal lensing, because it is close to the maxima of the spectra of all the selected metals.

Among the above metals, nickel and cobalt showed the most reliable and reproducible results (see Table 1). Thus, the further experiments with the HPLC–TLS system and data treatment dealt with PAR chelates of these metals. A routine chromatographic determination of Co^{2+} and Ni^{2+} as their PAR chelates with a conventional spectrophotometric detector under the conditions similar to our case resulted in the limits of detection of $7 \cdot 10^{-7}$ and $2 \cdot 10^{-5}$ M, respectively [10]. Repeatability standard deviation for spectrophotometric detection of both metals (by peak heights) was 5% (n=5).

3.3. Noise elimination

Even our first experiments with thermal lens detection in HPLC showed us that the high sensitivity of the detector to fluctuations of the mobile phase flow-rate could result in considerably degraded analytical characteristics of the procedures to be developed. The major source of noise is the fluctua-

tions generated by the pump although other components of the chromatographic system can also distort the signal.

As a result, the limits of detection of cobalt and nickel by thermal lensing without any data treatment were $5 \cdot 10^{-7}$ and $3 \cdot 10^{-5}$ M, respectively. Repeatability of determination is characterised by R.S.D. 20–25%. A comparison with spectrophotometric data evidently shows that such results are unacceptable.

To solve this problem, we selected an approach based on filtering the obtained data using the fast Fourier transform. This approach could give the best results for the system in question because the noise is determined by periodical fluctuations. Moreover, the frequencies corresponding to noise constituents (pumping and convection in the flow cell) differ significantly from the signal frequencies (chromatographic peaks); see the upper image of Fig. 3.

The filtering procedure can be divided into three stages: (1) calculation of a Fourier spectrum of the original data array FS (forward Fourier transform);

(2) calculation of a smoothed Fourier spectrum FS* (primary noise elimination), i.e. separation of the frequencies bearing any useful information from the spectrum using a special filtering function: multiplication of all the elements of FS by a numerical filter: FS*=FS×f; and (3) the backward Fourier transform of FS* giving a smoothed data array. The filtering function was the following, see Fig. 4 [5]:

$$f(n,k_1 k_2)$$

$$= \begin{cases} 1, n \le k_1; m - k_1 \le n \le m \\ \exp(-(n - k_1)^2 / k_2), k_1 \le n \le m/2 \\ \exp(-(m - n - k_1)^2 / k_2), m/2 \le n \le m - k_1 \end{cases} \quad (3)$$

Here, m is the number of points (frequencies) in the Fourier spectrum; n is the ordinal of a frequency in the spectrum ($1 \le n \le m$); and k_1 and k_2 are empirical parameters defining the widths of non-filtered edges and the half-width of the Gaussian pass band of the filter, respectively.

The first parameter k_1 defines the range of frequencies in a Fourier spectrum that are processed. This parameter is responsible for eliminating the noise with frequencies that significantly differ from
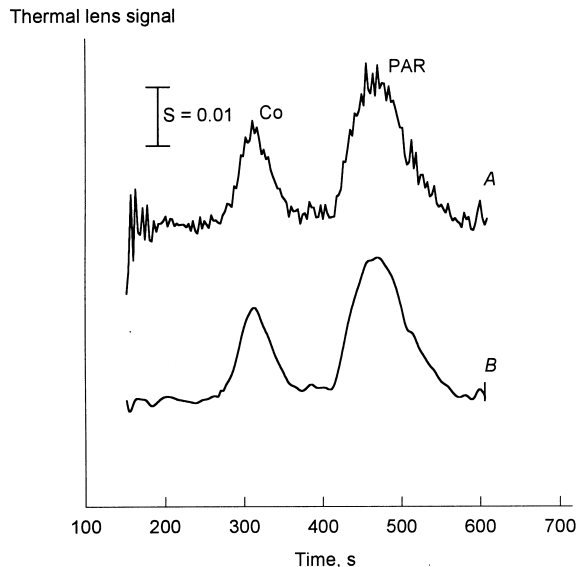
Thermal lens signal

Fig. 3. Peaks of cobalt(II) ($1 \cdot 10^{-7}$ M) chelates with PAR ($4 \cdot 10^{-5}$ M) (A) before smoothing (as detected by the thermal lens detector) and (B) after handling with the developed software. Filtering function parameters $k_1 = 0$ and $k_2 = 55$. Thermal lens detector: working wavelength 514.5 nm. Pump power in the cell 40 mW. A Nucleosil 10 SB 50×4.6 mm column; flow-rate 1.2 ml min^{-1}; eluent: 50 mM NaClO$_4$, 1 mM EDTA, 40% (v/v) acetonitrile.
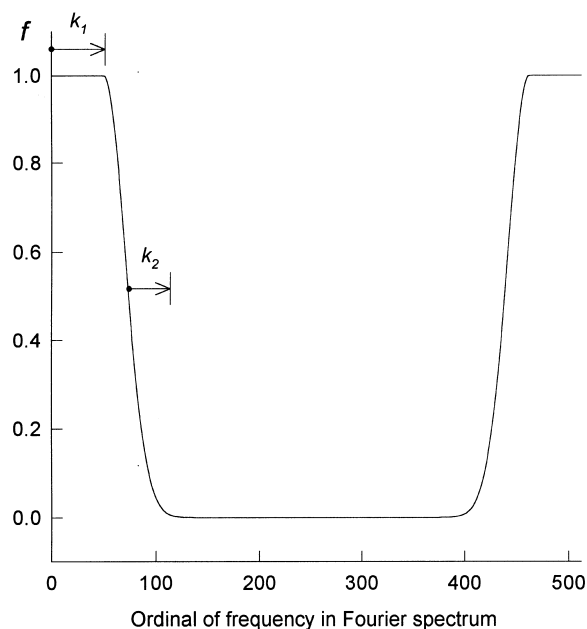

Fig. 4. Image of filter function f(n, k_1, k_2) used for smoothing chromatograms for m=512; see the text for variable definitions.

the frequencies of chromatographic peaks (like a short-term baseline noise or spurious points and a long-term baseline drift). Thus, if k_1 is too large, all the data in the original spectrum are not smoothed. The second parameter k_2 defines how one should treat the frequencies that are close to those of chromatographic peaks (like pump pulsation or convection beats). Large values of k_2 (very wide Gaussian edges, nearly no cutting of neighbouring frequencies) result in minor changes in curve shape leaving the noise unprocessed, The minimum value $k_2 = 1$ (nearly a rectangular-step filter) results in a sine-wave shape of the smoothed curve because all the neighbouring frequencies (including information-bearing data) are roughly cut off and only few frequencies remain in the middle of the Fourier spectrum.

In our experiments, the selection of k_1 and k_2 was made visually (fully resolved and noiseless Gaussian peaks) and resulted in $k_1 = 0$ and $k_2 = 50$–70 as the optimum. As an illustration, images of a chromatogram before and after the filtering procedure with the optimum parameters are shown in Fig. 3. All of the performance characteristics, which are discussed below, were calculated using filtered data.

3.4. Determination of metals

The comparison of the limits of detection of cobalt(II) and nickel(II), see Table 1, shows that the former shows greater sensitivity using both areas and heights as analytical signals. This can be accounted for higher molar absorptivity of the cobalt(II) chelate at 514.5 nm (see Table 2) and larger washout in the case of nickel(II) chelate. Thus, thermal lensing allowed an increase in the sensitivity by 1.5 orders for cobalt and by 2 orders for nickel.

Selectivity of the determination was tested by treating a set of five replicate experiments with a model mixture containing Co^{2+} and Ni^{2+} ($1 \cdot 10^{-5}$ M each) and PAR ($4 \cdot 10^{-5}$ M). The concentration of the reagent was selected so that its peak could be neglected (peak height and area comparable to the values of the baseline fluctuations). A chromatogram is shown in Fig. 5. The experiments showed that the peaks of cobalt(II) and nickel(II) are fully resolved and they do not affect the metrological characteristics of one another.
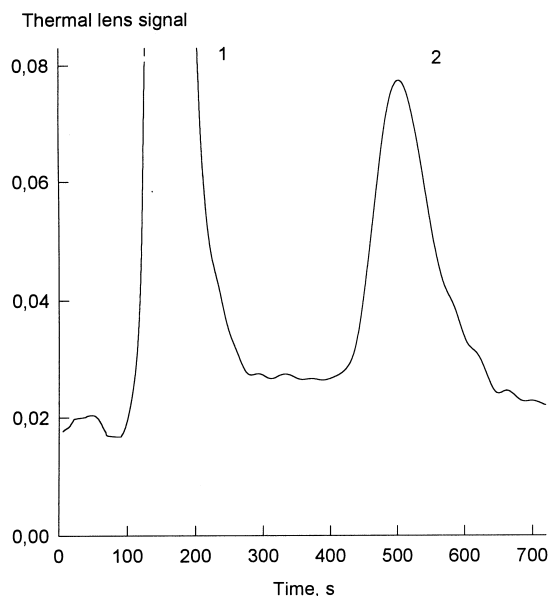

Fig. 5. Chromatogram of a solution containing chelates of (1) Co^{2+} and (2) Ni^{2+} (with concentrations of $1 \cdot 10^{-5}$ M) with PAR (total concentration of $4 \cdot 10^{-5}$ M). Thermal lens detector: working wavelength 514.5 nm. Pump power in the cell 40 mW. A Nucleosil 10 SB 50×4.6 mm column; flow-rate 1.2 ml min^{-1}; eluent: 50 mM NaClO$_4$, 1 mM EDTA, 40% (v/v) acetonitrile.

The comparison of the data on repeatability and reproducibility of the results (Table 1) shows that the precision of thermal-lens detection is similar to that of conventional spectrophotometry.

To obtain a more profound picture, we attempted to work with several other metals. We prepared three replicate series of solutions with $1 \cdot 10^{-5}$ M of Fe^{2+}, Cu^{2+}, and Pb^{2+} and PAR ($4 \cdot 10^{-5}$ M). All the chelates showed intense chromatographic peaks. Retention times, heights, and areas for these metals are summarised in Table 2. Metrological characteristics for these complexes were not calculated; however, the areas and heights of peaks are coincident with the molar absorptivities of the tested chelates (Table 2).

3.5. Filtering algorithm in HPLC–spectro-photometric applications

The proposed algorithm has no limitations on the method of detection and, provided the filter function is appropriate, can be used in treating any ex-

Table 2
Molar absorptivities and characteristics of chromatographic determination of metals as PAR chelates with a thermal lens detector ($P = 0.95$)

Metal	ϵ $(10^4 \, \text{l mol}^{-1} \, \text{cm}^{-1})$	c (M)	t'_R (s)	h (arb. units)	S (arb. units)	n
Co(II)	17	$5 \cdot 10^{-6}$	230 ± 6	0.24 ± 0.01	14 ± 2	5
Ni(II)	11	$2 \cdot 10^{-5}$	420 ± 10	0.32 ± 0.02	35 ± 3	5
Fe(II)	–	$1 \cdot 10^{-5}$	190 ± 10	0.24 ± 0.03	15 ± 2	3
Cu(II)	9	$1 \cdot 10^{-5}$	520 ± 10	0.05 ± 0.01	8 ± 1	3
Pb(II)	5	$1 \cdot 10^{-5}$	460 ± 10	0.14 ± 0.02	24 ± 2	3

Pump laser wavelength, 514.5 nm; pump power, 40 mW; Nucleosil 10 SB 50×4.6 mm column; flow-rate 1.2 ml min^{-1}; eluent: 50 mM NaClO$_4$, 1 mM EDTA, 40% (v/v) acetonitrile.

perimental chromatograms. In this study, it was expedient to compare its possibilities in HPLC for thermal lensing and conventional spectrophotometric detection. In the latter case, the contribution of the pulses of the mobile phase is much less significant than in the case of TLS, and the intensity of periodical constituents of the signal is low. Thus, filtering spectrophotometric data is less efficient than in HPLC–TLS: it results in the limits of detection by 0.5–1.0 orders instead of 1.5–2.0 orders in the case of thermal lensing.

3.6. Comparison of approaches to the data treatment

Thus, it was shown that detection limits calculated from peak areas are lower than the values from peak heights. In our opinion, it can be accounted for by a much weaker effect of peak broadening on areas than heights. Moreover, calculation of detection limits from peak areas is more appropriate. When calculating the limits of detection from peak heights, the standard deviation of the baseline is taken as a standard deviation of the blank: Thus, according to 3σ-criterion, a concentration is lower than the limit of detection if the height of the corresponding peak is lower than tripled background fluctuations. However, the peak remains visible because its shape and width dramatically differ from the shape and width of a single background fluctuation. The calculation method based on peak areas involves two parameters (height and width), thus making the numerical image closer to the real picture.

These speculations can be illustrated by the comparison of the limits of detection of cobalt and nickel (Table 1). The calculation by the peak heights results

in the difference in the limits of detection by the order of magnitude, whereas the approach based on peak areas shows that the limit of detection of cobalt is only three times lower than that of nickel. The latter value is much closer to the ratio of the molar absorptivities of their chelates with PAR at the working wavelength ($\epsilon_{Co}/\epsilon_{Ni} \cong 1.5$, $\lambda = 514.5$ nm). Thus, the effect of broadening of a peak of nickel on its limit of detection is much lower.

4. Conclusions

Thus, our study showed that a combination of thermal lens spectrometry and HPLC requires new approaches to the data treatment. The approach based on the fast Fourier transform filters proved its usefulness. Its main advantage lies in the fact that it may be used with any detection systems that are affected by the discussed factors (convection, pump beats, etc.). Moreover, the approach to calculating the limits of detection by peak areas may be of use in any studies dealing with microamounts in the flow.

Our next efforts will be directed toward finding smarter filter functions and automation and integration of data treatment into thermal-lens detection software.

References

[1] A. Berthaud, Spectrochim. Acta Rev. 13 (1990) 11.
[2] E.S. Yeung, Chromatogr. Sci. 45 (1989) 117.
[3] V.I. Grishko, V.P. Grishko, I.G. Yudelevich, Lazernaya Analiticheskaya Termolinzovaya Spektroskopiya (Analytical Laser-Induced Thermal-Lens Spectroscopy), In-t Neorg. Khim. SO RAN, Novosibirsk, 1992.

[4] A.G. Abroskin, T.V. Belyaeva, V.A. Filichkina, E.K. Ivanova, M.A. Proskurnin, V.M. Savostina, Yu.A. Barbalat, Analyst 117 (1992) 1957.

[5] M.A. Proskurnin, Cand. Sci. (Chem.) Dissertation, Moscow State University, Moscow, 1993.

[6] Z. Rozenzweig, E.S. Yeung, Appl. Spectrosc. 47 (1993) 1175.

[7] E.F. Simo-Alfonso, G. Ramis-Ramos, J.M. Ramis-Ramos, J.M. Estrella-Ripon, L. Hernandes-Geurra, V. Cedra-Martim, Quim. Anal. 9 (1990) 245.

[8] E.F. Simo-Alfonso, Y. Martin-Biosca, M.C. Garcia-Alvarez-Coque, G. Ramis-Ramos, Termochim. Acta 219 (1993) 53.

[9] C.E. Buffet, M.D. Morris, Anal. Chem. 54 (1982) 1824.

[10] I.P. Alimarin, E.N. Shapovalova, E.M. Basova, T.A. Bol-'shova, Zavod. Lab. 56 (1990) 11.